Regenerative Therapy 27 (2024) 434–444

Contents lists available at ScienceDirect

Regenerative Therapy

journal homepage: http://www.elsevier.com/locate/reth

Original Article

pH responsive fabrication of PVA-stabilized selenium nano formulation encapsulated with luteolin to reduce diabetic ureteral injury by decreasing NLRP3 inflammasome via Nrf2/ARE signaling

Qiang Jing [a], Fan Liu [a], Weitao Yao [b], Xuhui Zhang [a, *]

[a] Department of Urology, First Hospital of Shanxi Medical University, Taiyuan 030000, China
[b] Shanxi Medical University, Taiyuan 030000, China

ARTICLE INFO

Article history:
Received 1 March 2024
Received in revised form
1 April 2024
Accepted 11 April 2024

Keywords:
Luteolin
LT-SeNPs
Streptozotocin
Ureteral injury
Diabetics

ABSTRACT

Diabetic ureteral injury (DUI) is a condition characterized by damage to the ureter, causing functional and morphological changes in the urinary system, which have a significant impact on a quality of life and requires appropriate medical treatment. The present study describes to novel design of luteolin (LT), a type of natural flavonoid, encapsulated selenium nanoparticles (Se NPs) to attain therapeutic potential for DUI. The physico-chemical characterizations of prepared Se NPs have benefitted zeta potential (−18 mV) and particle size (10–50 nm). *In vitro* assays were demonstrated the potential of LT-SeNPs by HEK 293 cells stimulated by STZ for DUI. Cytotoxicity assays on HEK 293 and NIH-3T3 showed >90% cell viability, which demonstrates the suitability of the nanoformulation for DUI treatment. The LT-SeNPs significantly inhibits the NLRP3 inflammasome through Nrf2/ARE pathway, which benefits for DUI treatment. The developed LT-SeNPs could be an effective formulation for the DUI therapy.

1. Introduction

To prevent or slow the progression of diabetic nephropathy, renal disease, or ureteral inflammation, glycemic control should be prioritized [1]. Recent days, diabetes mellitus (DM) is the most common chronic metabolic illness. Diabetic wounds are a serious secondary consequence of type 2 diabetes that can cause permanent impairment and even death [2]. The one of the major complications caused by the DM was urinary complications were characterized by the sensation of bladder fullness, an increased capacity of the bladder, a decrease in bladder contractility, and an increase in post-void residual urine volume [3]. Ureteral injuries are very rare, making up less than 1% of all genitourinary trauma cases. Urinary tract injuries are extremely uncommon because of these changes, which reduce the retroperitoneum's diameter, mobility, and positioning, all of which serve to protect the ureter from the peritoneal contents, muscles, and bone in its immediate vicinity [4]. The several factors influence lower cystitis, prostatitis, and upper pyelonephritis, all of which result in urinary tract infections [5]. Worldwide, more women than men were diagnosed with this condition [6]. The diabetic ureteral disease may impair the activity of parasympathetic nitrergic pathways that treated with L-arginine which may leads to rise in nitric acid generation [7]. An effective inflammatory response to infection is mediated by inflammasomes, a kind of cytosolic multiprotein that serves as a scaffold for caspase-dependent activation, thereby encouraging cytokine synthesis and the release of proinflammatory cytokines [8]. Production of reactive oxygen species (ROS) has been associated to oxidative damage and has been shown to be a signal that activates the NLRP3 (nod-like receptor pyrin domain-containing 3) inflammasome, a key player in ureteral injury healing [9]. The anti-inflammatory gene is primarily regulated by the Nrf2 (NF-E2 p45-related factor 2)/ARE signaling pathways, which aid in suppressing inflammation's development [10]. Using its anti-inflammatory properties, Nrf2 influences the course of disease by controlling the expression of antioxidant genes and detoxifying enzymes such NADPH, NAD(P)H quinone oxidoreductase 1, glutathione peroxidase, ferritin, and heme oxygenase-1 (HO-1) [11]. By enhancing

* Corresponding author. Department of Urology, First Hospital of Shanxi Medical University, Taiyuan 030000, China.
E-mail address: xuhuizhangurology@126.com (X. Zhang).

Peer review under responsibility of the Japanese Society for Regenerative Medicine.

https://doi.org/10.1016/j.reth.2024.04.009

mRNA and protein expression, the HO-1 gene increases Nrf2, which mediates NF-κB signaling and attenuates inflammation [12]. According to the research, Nrf2 is vital for cellular homeostasis. When oxidative stress is under control, Nrf2 moves into the nucleus, where it connects with the ARE (antioxidant response element) and promotes the expression of HO-1 and other antioxidant genes [13]. Previously [14] reported that, LT as a potent stimulator of the Nrf2 signal, which plays a role in reducing inflammation by blocking the NLRP3 inflammasome. In this work, LT was utilized to treat inflammasomes in several organs, including the ureteral, by decreasing NLRP3 inflammasome through the Nrf2/ARE signaling pathway, which has previously been shown to be effective in treating ureteral injury caused by diabetes. The flavonoid luteolin LT (3′, 4′, 5, 7-tetrahydroxyflavone) is extensively distributed in foods like carrots, broccoli, celery, onion leaves, chinese celery, rosemary, bell peppers, and citrus fruits [15]. The glycosylated version of LT consists of three benzene rings: rings A and B are composed entirely of benzene, while ring C has an oxygen-carbon double bond at the 2–3 position and hydroxyl groups at carbon 5, 7, 3, and 4 play a crucial part in the drug's pharmacological activity [16]. They have been shown to have a wide range of biological effects, including those of antioxidant, anti-diabetic, and anti-cancer therapies [17]. These components may be useful in diagnosing DM and reducing the inflammation of the ureter caused by DM, as LT has been shown to be successful in treating DM [18]. There are drawbacks to using LT on its own, such as its poor solubility, physicochemical instability, and limited bioavailability [19]. Encapsulating with nanoparticles overcame these constraints and paved the path for more efficient delivering of drug at target sites, which improved treatment efficacy [20]. In this study the encapsulation of drug was carried out with the SeNPs they have been increased used in the field of anticancer agents and also used to carry drug because of its unique nature in chemo preventive effect [21]. They were also used in the treatment of diabetics [22]. The SeNPs were preferred because of their low toxicity, high bioavailability and novel therapeutic properties [23]. The selenium (Se) is an essential trace element found in kidney they may cause low acceptable level of intake and found to be toxic. The World Health Organization (WHO) recommends a daily dietary intake of 40 g Se/day for a healthy human life [24]. The toxicity can be overcome by converting it into the nanoparticles SeNPs it reduces the toxic level and widely used in all areas due to its high biological activity [25]. The SeNPs possess diverse effect on anti-inflammatory property these nanoparticles may be synthesized by various methods like physical, chemical and biological methods and these biological methods were consider safer, greener when compared to other methods [26]. The encapsulation of SeNPs to the LT which increase the thermal resistance and also enhance the ability of the retro gradation limits that provide the physiochemical properties needed for the encapsulation system [27].

The aim of the study to successfully load the LT into SeNPs and used for DUI by suppressing NLRP3 inflammasome. Where the LT were used to treat inflammation occurs in the brain [18], cardiac injury [13], cancer therapy [20]. At low concentrations, LT has been shown to inhibit the NLRP3 inflammasome [14]. The synthesis method of PVA, which differs from other green synthesis methods, was used to improve the activity of SeNPs when LT was encapsulated into it the encapsulation was done by ultrasonication method [28]. Optimizing the pH environment was another strategy for increasing the activity of LT-SeNPs by increasing the drug release capacity [29]. The study's primary objective was to compare and assess the efficacy of LT-SeNPs in treating diabetic DUI by inhibiting NLRP3 inflammasome by activating Nrf2/ARE signaling pathway.

2. Materials and methods

2.1. Materials

Luteolin was purchased from DASF Bio-Tech Ltd, (Nanjing, China). Sodium selenite, Polyvinyl Alcohol (PVA), Ascorbic acid was obtained from Sigma Aldrich (USA). The primary antibodies for NLRP3, Nrf2, and Caspase 1 were obtained from Santa Cruz Biotechnology (CA, USA). β-Actin was purchased from Bioworld Technology, HO-1 from Abcam. The SYRB Green Master Mix was obtained from Vazyme Biotech Co., Ltd. (Nanjing, China). DCFH-DA, (Beyotime, and shanghai, China), JC-1 Kit from (Solarbi, China).

2.2. Synthesis of SeNPs

The nanoparticles were synthesized with the safe and inexpensive approach by using a magnetic stirrer and maintained at 28 °C, 1 g of 100 mM sodium selenite was mixed with 50 mL of the distilled water. PVA solution with a concentration of 0.1% (W/V) was prepared by dissolving 0.05 g of PVA in 50 mL of distilled water while being stirred constantly for 15 min at 75 °C. After that sodium selenite was added to a PVA solution while constant stirring and then add ascorbic acid drop by drop, the fluid turned from colorless to orange, confirming the synthesis of SeNPs [30]. After further centrifugation, washing, and drying (at 50 °C), the resulting substance was then used for further studies, which was then stored for further use. The PVA was used as the stabilizer for the SeNPs [31].

2.3. Encapsulation of the LT to the SeNPs

The mixture with LT and SeNPs was suspended in 100% ethanol and subjected to ultrasonic vibrations at 25 °C for 30 min. The ultrasonication method was used to encapsulate LT into SeNPs through ultrasonic waves. After the process to separate the supernatant and the residue, the suspension was centrifuged at 2500 rpm for 15 min. After a second ethanol wash, the residue was centrifuged, and the resulting supernatant was collected. The absorbance of the combined supernatant was measured using a UV–Vis spectrophotometer at 350 nm. Then the concentration of the LT encapsulated was determined according to the calibration curve Where X is the concentration of LT (μg/mL), Y is the absorbance at 350 nm [27]. Characterization investigations, including UV–Vis, FTIR, Zeta potential, PDI (polydispersity index), TEM, were performed on the SeNPs and LT-SeNPs. Then the LT loaded SeNPs were further analyzed with the encapsulation efficiency, loading efficiency and drug releasing capacity and the pH responsive of the drug was evaluated using a dialysis method. In this method 10 mg of drug was dispersed in 5 mL of the phosphate buffer saline solution. The sealed bag was immersed in 40 mL of PBS buffer with pH 5, 6.5 and 7.4 and then they were shaken at 100 rpm at 37 °C at different time points the samples were collected and they were analyzed by UV spectrophotometer at wavelength of 220 nm. The overall mechanism was observed in Scheme 1.

2.4. In vitro cell culture

NIH3T3 and HEK 293 cells were cultured and maintained at DMEM (Dulbecco's Modified Minimum Essential Medium) which contains D-glucose and it was supplemented with 10% FBS (fetal bovine serum), 100 units/mL of penicillin and streptomycin that was maintained under 37 °C in 5% CO_2 environment [32]. The Chinese Academy of Sciences (in Shanghai, China) provided these cells. Both the cells were exposed to LT and LT-SeNPs and the cytotoxicity of the cell were analyzed. Then HEK 293 and NIH3T3 cells were treated with STZ (streptozotocin) which was dissolved in

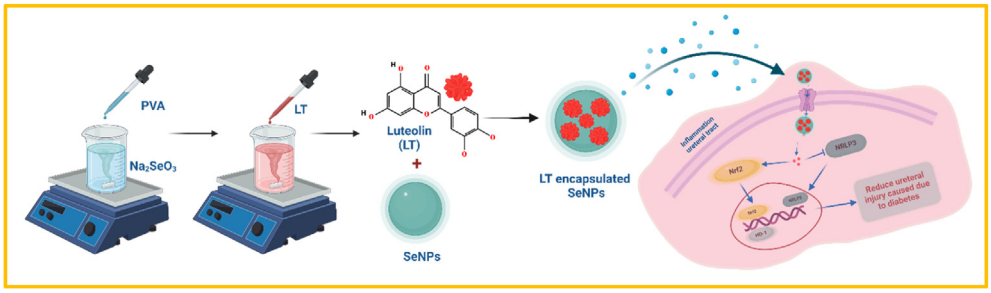

Scheme 1. This is a diagram that depicts the process of encapsulating Luteolin inside a selenium nanoparticle and how it works to cure gastric cancer.

a citrate buffer with a pH of 4.4. After the treatment of the cells with STZ they were extracted and washed with PBS (pH 7.4) and used for further analysis. The diabetes was induced in laboratory animals and cell lines by using *Streptomyces achromogenes* antibiotic (STZ) it was routine practice [33].

2.5. In Vitro cell cytotoxicity analysis

100 μL cell suspensions of HEK 293 and NIH3T3 were cultured in DMEM complete media and treated with STZ to generate diabetes were examined for cytotoxicity using MTT test. They were then seeded into the 96-well plates and left to grow in the incubator for a full 24 h. For 12 h, the cells were exposed to LT and LT-SeNPs at 25 μg/mL of concentration. After 2 h of incubation the media was discarded from the plates and added with 10 μL of the (5 mg/mL) MTT solution. After that 100 μL of DMSO was added, and the changes were observed by the microplate reader's absorbance at 570 nm. The drug LT-SeNPs at concentration 25 μg/mL was used for further studies as per the literature [34].

2.6. AO/EB staining for cell cytotoxicity

The cells HEK 293 and NIH3T3 were plated in 12 well plates and incubated for 24 h. They were treated with LT and LT-SeNPs at concentrations of 25 μg/mL for a day, after the treatment the cells were recovered and trypsinized. Further they were centrifuged at 1500 rpm for 5 min. The pellets were re-suspended in PBS buffer. The suspension of 10 μL was added with 1 μL of Acridine orange (AO) and 1 μL of Ethidium bromide (EB) were taken on the glass slide. Then observed under fluorescence microscopy (Olympus, Japan) at 200× [20].

2.7. qRT-PCR analysis

In order to evaluate real-time PCR using SYBR Green Master Mix, total RNA was extracted from the cells and reverse-transcribed into cDNA using PCR. Six-well plates were used to cultivate STZ-induced HEK 293 cell at ambient temperature. They were subsequently incubated for 24 h after being exposed to SeNPs, LT-SeNPs at 25 μg/mL of concentration. A total of 10 mL was used for each reaction, with 1 μL of cDNA, 5 μL of SYBR-Green reaction mix, 0.5 μL of antisense primer, and 3 μL of ddH_2O. Where Table 1 displays the primer sequence used to execute the reactions and calculate the relative changes [35].

2.8. Western blot analysis

The cell line HEK 293 was induced with STZ and used for the analysis of the Western blot. The proteins were separated by SDS-PAGE method and it was transferred to the PVDF membrane (Millipore, MA, USA). They were blocked with 3% of the BSA then incubated with the primary antibody used were Nrf2, HO-1, NLRP3, caspase-1, β-actin and incubated for overnight and washed thrice at TBST and further the band was incubated with the secondary antibody for 2 h at 28 °C and it was detected by using chemiluminescence imaging system (Shanghai, China) [36].

2.9. Measurement of ROS

For 20 min at 37 °C, 2, 7-dichlorodihydrofluorescein diacetate DCFH-DA, was added to cultures of STZ-induced HEK 293 cell line. Further the cell was treated with SeNPs, LT-SeNPs for 12 h at 28 °C, before being washed. Accuri C6 flow cytometry was used to quantify the levels of fluorescence [34]. To track variations in reactive oxygen species (ROS), the excitation and emission wavelengths are shifted from 485 nm to 530 nm.

2.10. Mitochondrial membrane potential assay

HEK 293 was stained with JC-1 Kit after STZ induction. Before the culture media was discarded, cells were seeded in a 12-well plate and treated with LT, LT-SeNPs for 24 h. In addition, 250 μL of the JC-1 fluorescent probe was given to the cells, and they were cultured for an additional hour at 37 °C. After measuring the fluorescence intensity with Accuri C6 flow cytometry, the culture media was rinsed three times with the buffer. The excitation and emission wavelengths of green fluorescence in J-monomers are 515 and 529 nm, respectively. Measurements of the ratio of green to red fluorescence were utilized to calculate the mitochondrial membrane potential. This ratio is used to track changes in the MMP and serves as an indicator of the health and function of the mitochondria. As in healthy cells, JC-1 aggregates and releases red

Table 1
The primers used for qRT-PCR Analysis.

Primer name	Forward primer	Reverse primer
NLRP3	5′-AACATTCGGAGATTGTGGTTGGG-3′	5′-GTGCGTGAGATTCTGATTAGTGCTG-3′
Nrf2	5′-GGGATGAGCTAGTGCTGATCTGG-3′	5′-AAACTTGCTCCATGTCCTGCTCTA-3′
HO-1	5′-TGCAGGTGATGCTGACAGAGG-3′	5′-GGGATGAGCTAGTGCTGATCTGG-3′
caspase-1	5′-TTACAGACAAGGGTGCTGAACAA-3′	5′-TGAGGAGCTGGAAAGGAAGAAAG-3′
β-Actin	5′-CATCCTGCGTCTGGACCTGG-3′	5′-TAATGTCACGCACGATTTCC-3′

fluorescence when the potential across the mitochondrial membrane is high. This is because the dye molecules are so close together. Contrarily, JC-1 stays monomeric and exhibits green fluorescence in cells when mitochondria are depolarized, which indicates mitochondrial damage [34].

2.11. Assay of cell apoptosis

After a day of incubation at 37 °C and 5% CO_2, STZ-induced to HEK 293 cell that were sown into 12-well plates. For 24 h, one set of cells was treated with SeNPs, LT-SeNPs, while the other group served as a control. All of the samples were run using flow cytometry (Merck Millipore, Germany) in triplicate to ensure accuracy of results [37].

2.12. Statistical analysis

In order to compile the data, we used GraphPad Prism 8.02 for statistical analysis. Statistical significance was set at the $P < 0.05$ level, and all data were presented using the mean SD format. One-way or two-way analysis of variance (ANOVA) followed by the Bonferroni post hoc test was used to compare the differences between the groups.

3. Result and discussion

3.1. Formation of the nanoparticles

The nanoparticles were prepared from sodium selenite by adding it with the reducing agent ascorbic acid, in this reaction the color changes have been occurred from colorless to brick red which denotes the formation of the SeNPs. The polymer PVA blend with the nanoparticle enhances the behavior of the nanoparticle by improving their structure and their morphology [38].

3.2. Encapsulation of the SeNPs

The SeNPs were added with different dosage of the LT that were analyzed under the UV-Spectrophotometer which says that increase in LT concentration increases the Encapsulation Efficiency which also increases the Loading Efficiency. After the loading and encapsulation efficiency further, we need to analysis the release of the LT from the nanoparticle. According to Fig. 1A we observed that the EE increases from 80 to 93% along with the increase in loading efficiency from 3.5 to 11% was shown in Fig. 1B. They were analyzed with the results of LT encapsulation in the literature [39]. After the LT was efficiently encapsulated into the SeNPs further the characteristics properties were analyzed. The LT release into the cells were estimated that is known as drug releasing capacity where LT used as control and LT-SeNPs encapsulated were used that shows increase in drug releasing capacity this was shown in Fig. 1C were the drug releasing may depend upon the type of the materials used to load, where the SeNPs acts as better carrier for the drug delivery [40]. The effect of pH of the drug release for LT-SeNPs was estimated pH 5, 6.5 and 7.4 were these SeNPs was sensitive to pH changes and from Fig. 1D observed that the drug release was faster at pH 5 when compared to pH 6.5 and releasing was slow at pH 7.4 where the 80% of drug released within 12 h and the changes was observed until 48 h hence it is proved that the stability of LT-SeNPs was reduced, resulting in more and faster drug released into the buffer this was similar to the silk fibroin encapsulated within selenium nanoparticles [41].

3.3. Characterization of LT-SeNPs

In the characterization study the UV–Visible absorption was observed from 200 to 800 nm. The maximum absorption was obtained at 290 nm (Fig. 2A), which is comparable to the synthesis of SeNPs with *Arabinogalactans* [42]. The absorption of LT was around

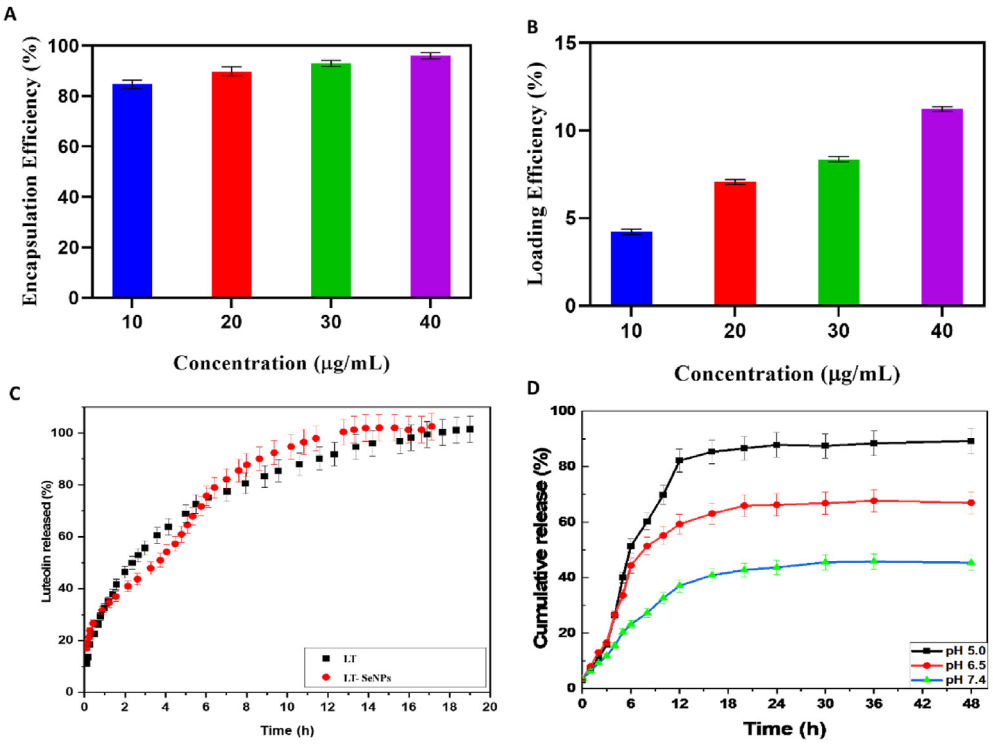

Fig. 1. Graph depicting the effect of LT on encapsulation efficiency as the concentration increases the EE% has been increased (A). Loading efficiency of the LT into SeNPs (B). Drug releasing capacity of the LT from selenium nanoparticles (C). The graph depicts the pH dependent LT-SeNPs release profiles in PBS (pH 5, pH 6.5 and pH 7.4) at various time intervals (D).

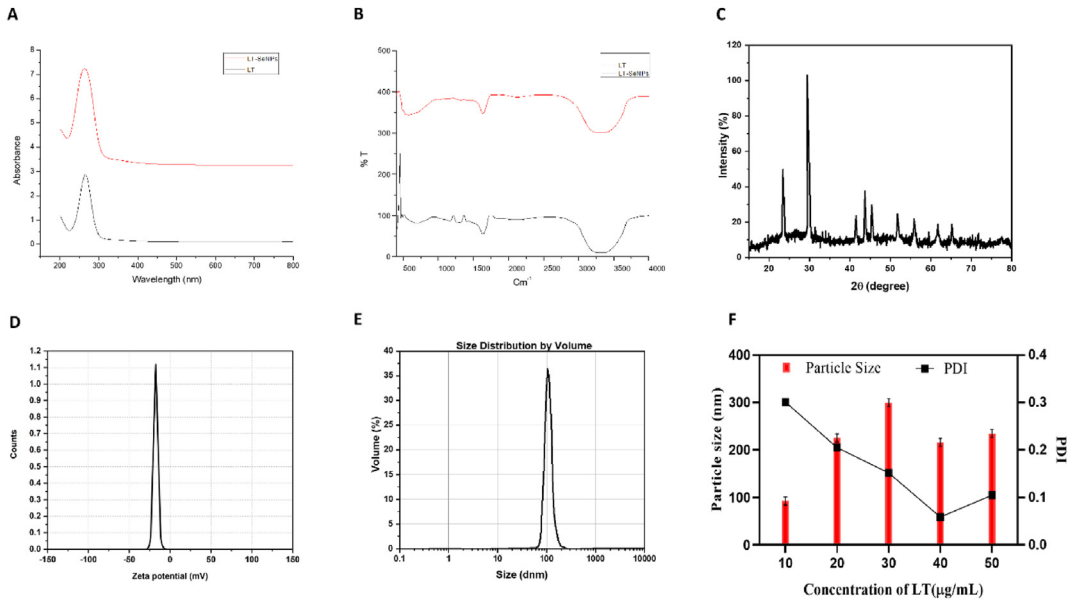

Fig. 2. The study of selenium nanoparticles analyzing UV–Visible spectrum of LT and LT-SeNPs (A). FTIR of LT and LT-SeNPs (B). XRD pattern of the SeNPs (C). Zeta-potential of the LT-SeNPs (D). PDI (E&F).

(250–346 nm) [43]. The band formed the confirmation of the LT and LT-SeNPs where the SeNPs shows broad UV range as per the literature and it also confirms the encapsulation of LT into SeNPs. The FTIR was observed between 4000 and 400 cm^{-1} the broad peak has been observed in between 3434 cm^{-1} [44]. Because of the presence of phenolic group, the observed FTIR spectra of LT revealed –OH vibration band at around 3431.6 cm^{-1}. The band at 1613.6 cm^{-1} was caused by C=O vibrations in the Central heterocyclic ring of LT. The band at 1200 cm^{-1} in Fig. 2B shows a C–N bond. After the nanoparticles formed the activity of the hydrogen bond becomes increases the shift of the band indicates the electrostatic interaction which leads to the formation of the stable rings [45]. The XRD demonstrates the crystallinity of the particle by displaying reflection peaks at (100), (101) that denote the formation of the SeNPs. The peaks of the reflections in Fig. 2C were similar to those found in the literature [25]. The Zeta potential of the LT-SeNPs was found to be –18 mV from Fig. 2D which was the similar results obtained when LT loaded to the SeNPs where, the zeta potential provides the information about the stability of the nanoparticles where the negative values show low aggregation which enhances the stability of the nanoparticle formed [46]. The zeta potential of the zein nanoparticles was found to be –11.11 mV was observed from Fig. 2D where, the zeta potential in negative effect shows high polydispersity index [20]. The PDI (polydispersity index) was 0.264, and a PDI less than 0.3 indicates that the SeNPs were loaded with flavonoids, as shown in Fig. 2E and F [47]. Once the drug encapsulated The TEM images shows that formed nanoparticles were found to be uniform and spherical in shape with the diameter ranges from 10 to 50 nm. The LU-SLNs were analyzed to the TEM which shows it was round in shape [48]. The structure of

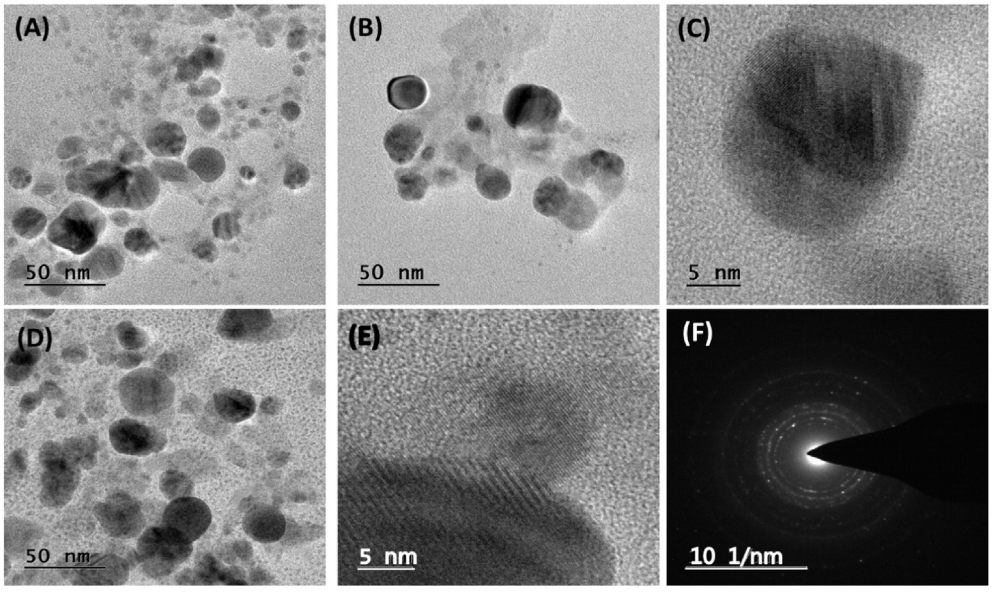

Fig. 3. Images of SeNPs using TEM (A). SeNPs coated with PVA (B&C). LT encapsulation with SeNPs (D& E). The created nanoparticle complex was demonstrated to exhibit selective area electron diffraction (SAED) in (F).

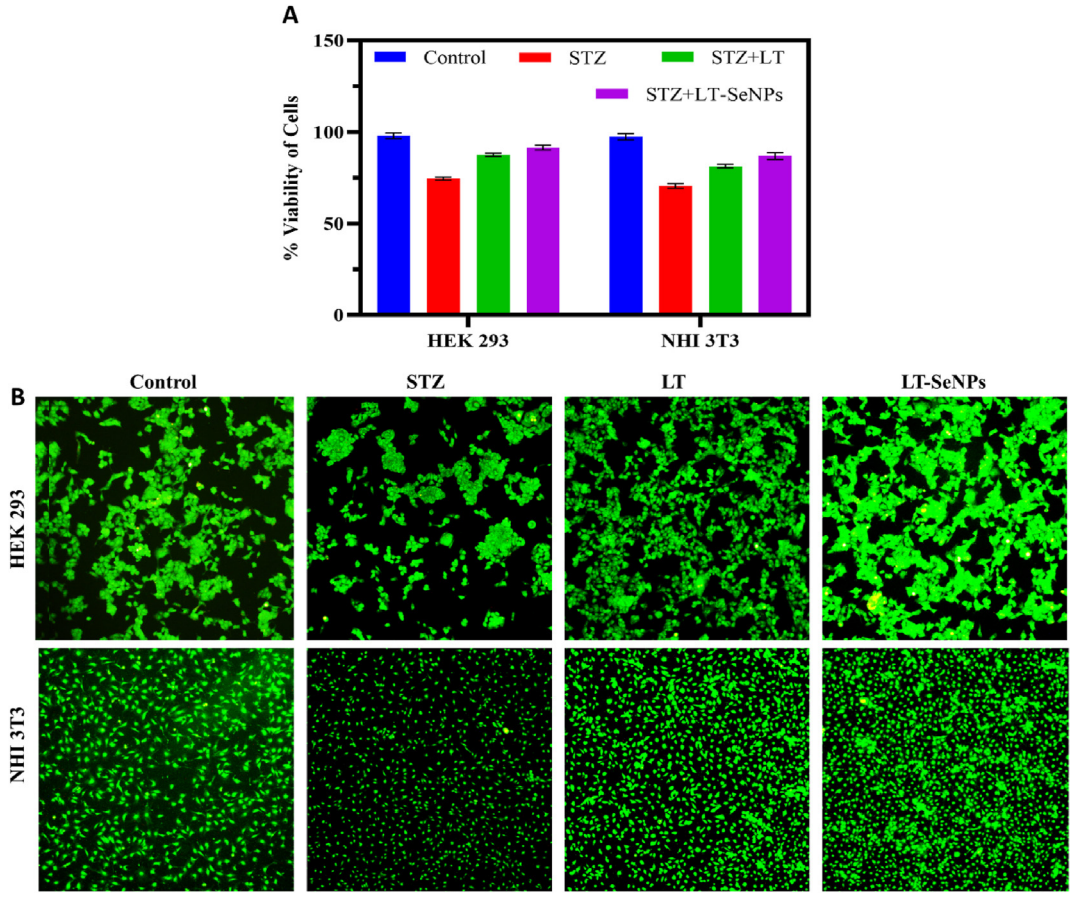

Fig. 4. The cytotoxicity of the cell lines HEK293 and NHI 3T3 was investigated using MTT assay for control, STZ-induced, and STZ-induced cell lines (A). AO/EB staining were carried out on the cell line and the changes of the cell line after treatment with the drug LT and LT-were observed were STZ induced model shows less cell viability when treated with the drug the percentage loss of cells has been reduced and the changes have been observed for 24 h interval and images were at 4× magnification (B).

the SeNPs was observed in Fig. 3A, where Fig. 3B and C represents the SeNPs coated with PVA and Fig: 3D&E represents the encapsulation of the SeNPs with the LT and Fig. 3F denotes the SEAD pattern of the clearly denotes the dimension, shape and topology of the formed nanoparticles. Where the SEAD pattern recorded diffraction spots or rings with interplanar spacing that was recorded as spherical in shape and this confirms the purity of the formed nanoparticles.

3.4. In Vitro cell cytotoxicity study by MTT assay

The viability of mitochondria was assessed by measuring their capacity to convert MTT salt into formazan product which provided a measure of the cell cytotoxicity [45]. The changes in the NIH3T3 and HEK 293 cells were observed. When the STZ was induced to the cell lines a decrease in mitochondrial dehydrogenase's effect on cell viability was observed. The LT and LT-SeNPs were used to treat the cell lines. Where LT treatment decreased STZ-induced diabetic in the cell, this finding suggests that LT-SeNPs is more effective than LT in preventing diabetes. According to the graph (Fig. 4A), the strong cell cytotoxicity in STZ-induced and when treated with LT and LT-SeNPs increased cell viability by up to 90%, proving to reduce diabetes levels. The LT-SeNPs has greater efficacy in treating cells than the LT [49]. When STZ is induced in HepG2 cells, similar results are observed, namely a decrease in cell viability. When NIT-1 cells were treated with streptozotocin (STZ), cell viability decrease [50].

3.5. AO/EB staining to analysis the cell viability

AO/EB staining assays was used to analysis the changes in the cell morphology. Where the live cells were stained with acridine orange (AO) in green color and dead cells were stained with ethidium bromide (EB) in red color. The cells induced with STZ show apoptosis (Fig. 4B), as do the cells treated with LT and LT-SeNPs, which were used to overcome the cell apoptosis caused by diabetics, and the obtained results confirm that it was effective in treating diabetics. Where the cells NIH-3T3 and HEK 293 they both shows effective while treating with LT-SeNPs. The similar results were obtained in the literature [51]. The MDA-MB-231 cells were treated with methanolic extract and aqueous extract and the changes were observed by using AO/EB staining and was found that methanolic extract show high toxicity when compared to the aqueous extract [52]. The morphological changes of the cell images were observed from the (Fig. 5) at various treatment. Where Fig. 5A represents the changes in the HEK 293 cell lines and Fig. 5B denotes the changes in the NIH-3T3 cell lines.

3.6. qRT-PCR analysis

To assess the feasibility of the new technology for analyzing miRNAs the q-PCR methods were used. The Nrf2 signaling pathway is the major regulator of antioxidant stress in animal cell lines by modulating the transcription genes that includes HO-1 [53]. We can see from the graph (Fig. 6) that the protein fold for Nrf2 has

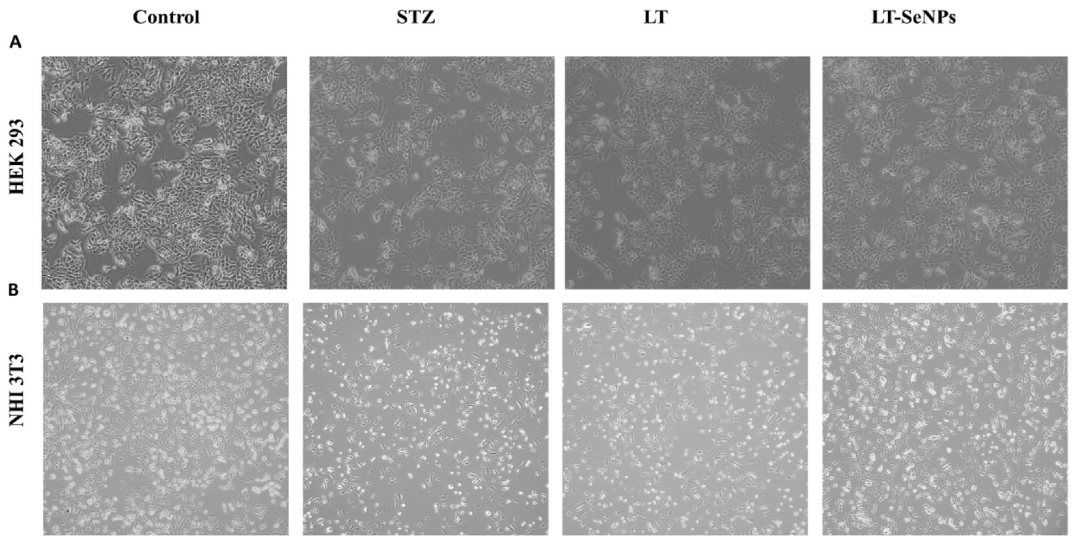

Fig. 5. The morphological alterations in the cell lines (HEK 293 and NHI 3T3) after treatment with STZ, LT, and LT-SeNPs are indicated and the images were at 4× magnification.

increased, confirming that these proteins suppress the NRLP3 inflammasome. According to the graph, Nrf2 increases by 0.9-fold while NRLP3 suppresses by 0.4-fold. These inflammasome may cause ureteral injury at high glucose conditions and hence they should be treated to reduce the inflammation. When comparing the activity of the drug LT and LT-SeNPs, the LT-SeNPs shows highly efficient inducing Nrf 2 protein expression and thus reduces the NLRP 3 inflammasomes by reducing diabetics. The pervious results have been shown to similar for the protein expression they are Nrf2, HO-1, NQO-1 that increases in protein expression which may tends to reduce NLRP3, ASC, Caspase-1 which was shown to be effective in treating spinal cord injury [54]. The other study shows that the glucose induced to the cells causes the activation of NLRP3 inflammasome where the compound LT used to reduce the glucose level thereby inhibiting the NLRP3 inflammasome [55].

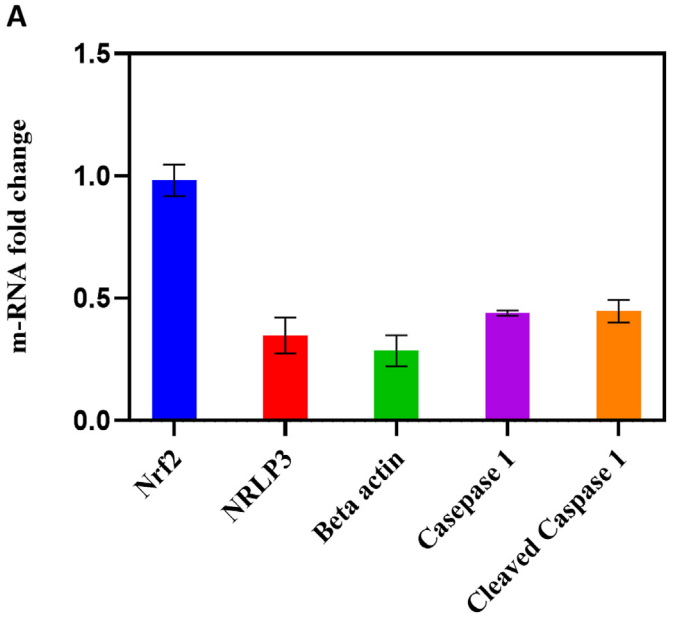

Fig. 6. qRT-PCR was used to determine relative mRNA levels were the relative genes Nrf2, NRLP3, Beta actin, Caspase 1 and cleaved caspase 1 shows the gene expression level; the bar graph represents the significance difference between groups and found the Nrf 2 activates which reduce NLRP3 inflammasome.

3.7. Western blotting assay

Protein concentration was determined by western blotting, in which the separated proteins were transferred to nitrocellulose paper and stained with primary and secondary antibodies. Fig. 7A shows the western blotting gel images. This study shows that LT-SeNPs are beneficial in treating DUI by decreasing NLRP3, and Cleaved caspase-1 expression. MPC-5 cells also demonstrate anti-apoptotic activity via suppressing the NLRP3 inflammasome [33]. While previous data reveal that the LT and LT-SeNPs have a significant capacity to diminish the ASC speck in the presence of high glucose, the STZ was induced in cell lines that showed a high degree of ASC speck production. The graph shows that the addition of LT-SeNPs to STZ-treated cells has been shown to be efficient in suppressing the NLRP3 inflammasome and halting the development of ureteral damage [56]. Fig. 7B depicts the HO-1 level after treatment, where HO-1 increases. The caspase 1 level is shown in Fig. 7C, and the cleaved caspase 1 level is shown in Fig. 7D after treatment the level has been reduced. The NLRP3 level in Fig. 7E has been decreased, whereas the Nrf2 level in Fig. 7F has been increased when treated. This supports the suppression of NLRP3. Melatonin (MT) was also studied for its anti-inflammatory effects following spinal cord injury, and it was found to activate the Nrf2/ARE pathway, which typically suppresses the NLRP3 pathways [57]. Studies with LT that were treated to activate Nrf2 and subsequently decrease NRLP3 inflammasome showed similar results. The experiment could be reversed by employing ML385 to silence Nrf2 [36].

3.8. Measurement of ROS generation

In diabetics, reactive oxygen species (ROS) play a crucial role in the initiation of apoptosis. Apoptosis is further activated when cytochrome *c* is released when MMP is disrupted by ROS [58]. The anti-oxidant drug LT can block ROS production caused by HG [34]. The STZ-induced decrease in reactive oxygen species (ROS) levels may shield cells from oxidative stress [59]. The DCFH-DA technique was used to detect ROS; this compound diffuses across the cell membrane and is then degraded by intracellular esterases to DCFH-

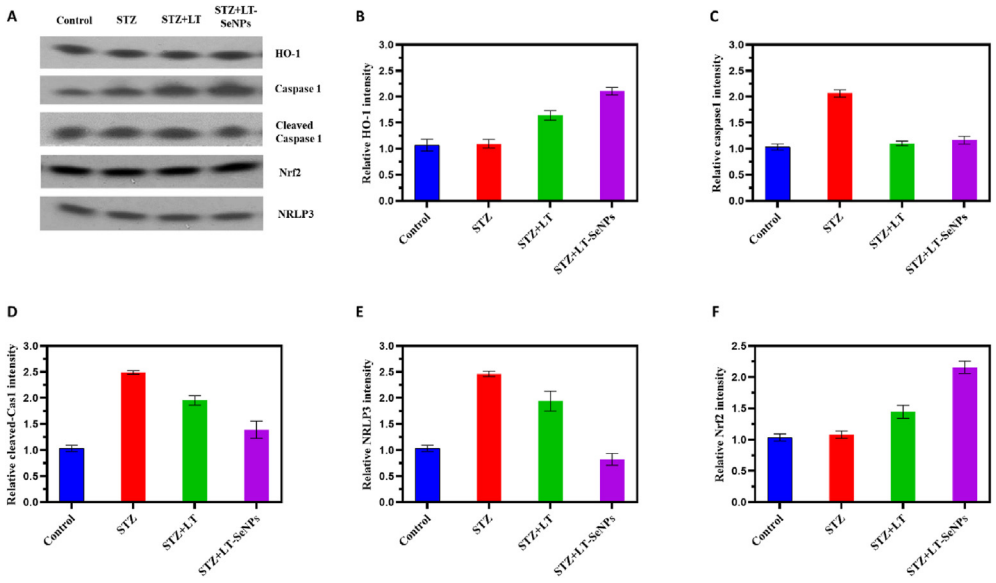

Fig. 7. Western blotting was used to examine the expression of inflammasome on the HEK 293 cell line where (A) represents the gel image. Relative intensity was estimated for HO-1 (B), Caspase 1(C), cleaved caspase 1(D), Nrf2 (E), NLRP3 (F).

DA [60]. The graphical representation of ROS (Fig. 8A) confirms that the LT-SeNPs successfully inhibited ROS production, which in turn suppressed NLRP3 inflammasome activation. Fig. 8B shows that after STZ induction, ROS levels in the cell line rise; however, when the drug LT is added to the cell line, MMP activity recovers and even increases, protecting the cells from apoptosis. Furthermore, LT-SeNPs exhibits higher activity than the drug LT alone. Previous research on RIN-5F pancreatic β-cells [59] and found similar action. In addition to its use in preventing and treating neurodegenerative diseases, LT has been shown to be effective in treating neuronal damage [61]. LT is crucial because it induces several different antioxidative genes, which work together to scavenge ROS and prevent the NRLP3 inflammasome from act [62].

3.9. Analysis of mitochondrial membrane potential activity

When cellular levels of matrix metalloproteinase, an enzyme essential for cellular function maintenance, drop, the apoptotic pathway is activated [63]. Fig. 8C represents the graphical representation of the cell's MMP level, and Fig. 8D represents the activity of cells during treatment. As the quantity of STZ-induced cells drops, it becomes clear that these cells were pushed into apoptosis by the presence of glucose. To prevent cell death, apoptosis, LT is used to lower the cell blood sugar levels, which in turn increases the quantity of mitochondrial membrane protein. Whereas prior research has shown that the drug LT can restore MMP collapse and protect membranes from damage, LT-SeNPs have been shown to be

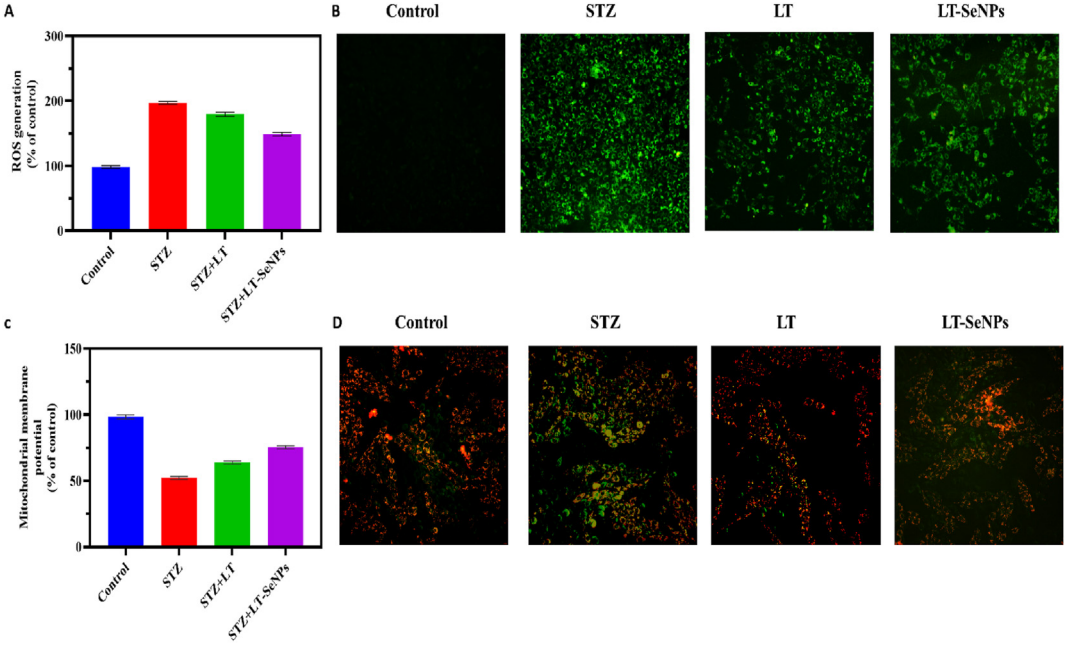

Fig. 8. In the HEK 293 cell line, LT-SeNPs has the ability to inhibit the generation of ROS where, the graphical representation of the ROS among control and treated with LT and LT-SeNPs (A). The HEK 293 ROS cells images (B). Mitochondrial membrane potential was determined using JC-1 staining where, the graphical representation of the MMP indicating that LT-SeNPs are effective in treating NRLP3 inflammasome (C). MMP of HEK 293 in cell images (D), where the images (B) and (D) were shown at 10× magnification.

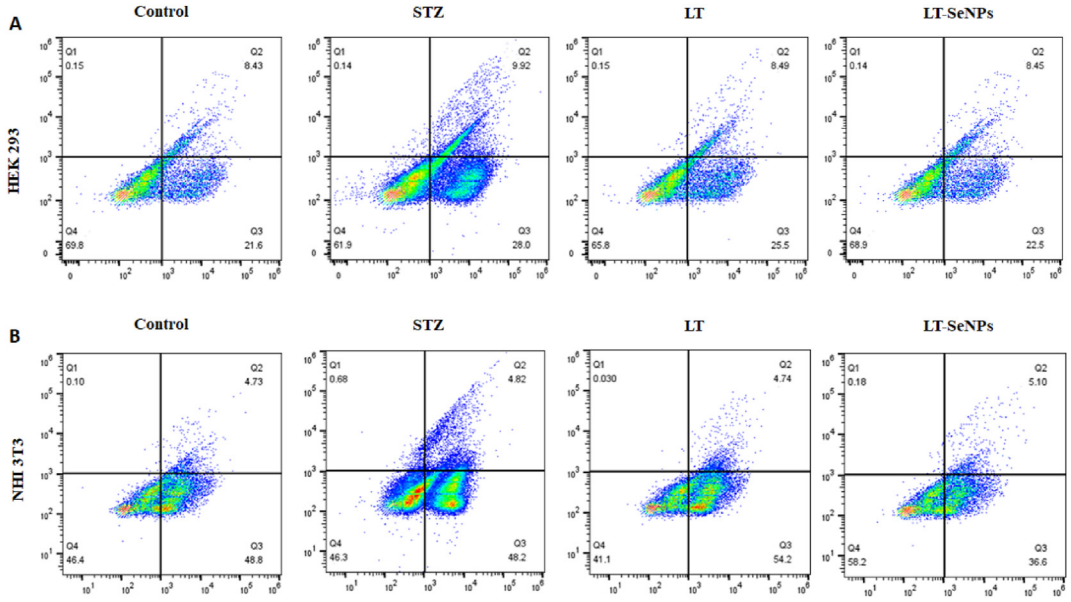

Fig. 9. LT-SeNPs reduced NLRP3 inflammasome by activating the Nrf2 signaling pathway, according to flow cytometer analysis where the expression of flow results for HEK293 (A). Flow results for NHI 3T3 (B).

more successful in treating the condition [64]. The JC-1 dye indicates the extent to which damage has occurred to the mitochondrial membrane.

3.10. Analysis of cell apoptosis by using flow cytometer

Drugs LT and LT-SeNPs were tested for their ability to prevent DUI using a flow cytometer. Both the NIH3T3 and HEK 293 cell lines showed remarkable sensitivity to the LT's anti-diabetic effects. Treatment of ureteral damage is improved when LT is encapsulated in SeNPs [55]. Treatment with LT and LT-SeNPs, which act on the cell to reduce the level of STZ and thus cell apoptosis, was found to be effective in treating DUI (Fig. 9). Where, Fig. 9A represents the apoptosis rate of HEK 293 and Fig. 9B, represents the changes in apoptosis of NIH3T3. Previous research has shown that ZnO quantum dots suppressed apoptosis in HeLa and HEK-293T cells [37]. SPS-SeNPs which induce apoptosis in A375 human melanoma cells [65]. From the evidences of the other studies the LT-SeNPs was shown to be effective in treating DUI caused due to the diabetics. The LT has effect on several diabetic's base complications such as diabetic cardiomyopathy, diabetic neuropathy, diabetic cataract and diabetic encephalopathy. Where they also proved to be effective in treating NLRP3 inflammasome [34]. The DUI was cured by using LT-SeNPs was studied HEK 293 cells line by inducing the diabetics in it and it was shown to be high effective on the treatment with the drug LT-SeNPs [20]. In this case, the NIH3T3 cell line represents embryonic fibroblasts originally from mice. For the purpose of research, it is a typical cell line. For biocompatibility testing and, more specifically, inflammatory assays, they were utilized. Human embryonic kidney cell lines (HEK 293) were used in our study on ureteral damage; thus, we chose these cell lines to analyze the functional studies of the NLRP3 inflammasome and validate the activation of the Nrf2/ARE signaling pathway. To assess the biocompatibility, cellular uptake, anti-inflammatory properties, and modulation of signaling pathways of the LT-SeNPs in treating DUI, the NIH3T3 and HEK 293 cell lines were selected. The LT-SeNPs improve the treatment by increasing the drug's efficacy and decreasing the drug's release times. Further the ROS, protein expression and apoptotic studies were studied to analysis the efficacy of the drug in treating DUI and found that LT was efficient in treating diabetics by acting as the ROS scavenger that suppress the inflammasome where the NLPR3 need ROS sensitive pro-inflammatory signal and it block ROS scavenger. The LT was known to be a good anti-oxidant and suppress the activation of NLRP3 [66]. Where the LT loaded with SeNPs shows better results in suppressing the NLRP3 inflammasome.

4. Conclusion

In summary, pH-responsive drug delivery system was developed by the fabrication of SeNPs encapsulated with LT using PVA-template. The results of this study show that the preparation of Se NPs has promising therapeutic action for DUI treatment. Here, we examined and established the regeneration potential of LT-SeNPs on STZ-induced HEK 293 cell model. The *in vitro* outcomes established that LT-SeNPs synergistically reduced the cell apoptosis and increased regeneration potential after DUI. The results of qRT-PCR and western blotting confirmed that significant decrease of NLRP3 expressions after LT-SeNPs administration. The therapeutic benefits of LT-SeNPs were found to be mediated through the activation of the Nrf2/ARE signaling pathway, which led to the downregulation of NLRP3 expression and reduce DUI. The results of this study demonstrated that the preparation of LT-loaded nanoformulation has promising action on treatment of DUI.

Funding

Scientific Research Project of Shanxi Provincial Health Commission (Grant No. 2023050) Shanxi basic research project (Grant No. 202103021224403).

Declaration of competing interest

The authors compete that there is no conflict of interest.

References

[1] Donate-correa J, Martín-núñez E, Muros-de-fuentes M, Mora-fernández C, Navarro-gonzález JF. Inflammatory cytokines in diabetic nephropathy. J Diabet Res 2015;2015.

[2] Saeedi P, Petersohn I, Salpea P, Malanda B, Karuranga S, et al. Global and regional diabetes prevalence estimates for 2019 and projections for 2030 and 2045: results from the International diabetes Federation diabetes atlas. Diabetes Res Clin Pract 2019;157:107843. https://doi.org/10.1016/j.diabres.2019.107843.
[3] Paper O. Changes in Alpha1-Adrenoceptor and NGF/proNGF pathway: a possible mechanism in diabetic urethral dysfunction. 2014. p. 344–51. https://doi.org/10.1159/000355711.
[4] Brown RL, Falcone RA, Garcia VF. Genitourinary tract trauma. In: Pediatric Surgery; 2012. p. 311–25. https://doi.org/10.1016/B978-0-323-07255-7.00021-0. 2-Volume Set: Expert Consult - Online and Print.
[5] Zacchè MM, Giarenis I. Therapies in early development for the treatment of urinary tract inflammation. Expet Opin Invest Drugs 2016;25(5):531–40. https://doi.org/10.1517/13543784.2016.1161024.
[6] Rusz A, Pilatz A, Wagenlehner F, Linn T, Diemer TH, et al. Influence of urogenital infections and inflammation on semen quality and male fertility. World J Urol 2012;30(1):23–30. https://doi.org/10.1007/s00345-011-0726-8.
[7] Torimoto K, Fraser MO, Hirao Y, De Groat WC, Chancellor MB, Yoshimura N. Urethral dysfunction in diabetic rats. J Urol 2004;171(5):1959–64. https://doi.org/10.1097/01.ju.0000121283.92963.05.
[8] Ding Y, Ding X, Zhang H, Li S, Yang P, Tan Q. Relevance of NLRP3 inflammasome-related pathways in the pathology of diabetic wound healing and possible therapeutic targets. Oxid Med Cell Longev 2022;2022. https://doi.org/10.1155/2022/9687925.
[9] ru Li J, Xu HZ, Nie S, Peng YC, Fan LF, Wang ZJ, et al. Fluoxetine-enhanced autophagy ameliorates early brain injury via inhibition of NLRP3 inflammasome activation following subrachnoid hemorrhage in rats. J Neuroinflammation 2017;14(1):1–14. https://doi.org/10.1186/s12974-017-0959-6.
[10] Ahmed SMU, Luo L, Namani A, Wang XJ, Tang X. Nrf2 signaling pathway: pivotal roles in inflammation. Biochim Biophys Acta, Mol Basis Dis 2017;1863(2):585–97. https://doi.org/10.1016/j.bbadis.2016.11.005.
[11] Braun S, Hanselmann C, Gassmann MG, dem Keller U, Born-Berclaz C, Chan K, et al. Nrf 2 transcription factor, a novel target of keratinocyte growth factor action which regulates gene expression and inflammation in the healing skin wound. Mol Cell Biol 2002;22(15):5492–505. https://doi.org/10.1128/mcb.22.15.5492-5505.2002.
[12] Sangokoya C, Telen MJ, Chi JT. microRNA miR-144 modulates oxidative stress tolerance and associates with anemia severity in sickle cell disease. Blood 2010;116(20):4338–48. https://doi.org/10.1182/blood-2009-04-214817.
[13] Baiyun R, Li S, Liu B, Lu J, Lv Y, Xu J, et al. Luteolin-mediated PI3K/AKT/Nrf2 signaling pathway ameliorates inorganic mercury-induced cardiac injury. Ecotoxicol Environ Saf 2018;161(May):655–61. https://doi.org/10.1016/j.ecoenv.2018.06.046.
[14] Nam M, Lee Y, Wu D, Pae M. Luteolin inhibits NLRP3 inflammasome activation via blocking ASC oligomerization. J Nutr Biochem 2021;92:108614. https://doi.org/10.1016/j.jnutbio.2021.108614.
[15] Zhang C, Zhang Y, Hu X, Zhao Z, Chen Z, Wang X, et al. Luteolin inhibits subretinal fibrosis and epithelial-mesenchymal transition in laser-induced mouse model via suppression of Smad2/3 and YAP signaling. Phytomedicine 2023;116:154865. https://doi.org/10.1016/j.phymed.2023.154865.
[16] Talib WH, Alsalahat I, Daoud S, Abutayeh RF, Mahmod AI. Plant-derived natural products in cancer research: extraction, mechanism of action, and drug formulation. Molecules 2020;25(22). https://doi.org/10.3390/MOLECULES25225319.
[17] Chen L, Cheng H, Liao C, Kuan Y, Liang T. Luteolin improves nephropathy in hyperglycemic rats through anti-oxidant, anti-inflammatory, and anti-apoptotic mechanisms. J Funct Foods 2023;102(February):105461. https://doi.org/10.1016/j.jff.2023.105461.
[18] Chen LY, Cheng HL, Liao CK, Kuan YH, Liang TJ, Tseng TJ, et al. Luteolin improves nephropathy in hyperglycemic rats through anti-oxidant, anti-inflammatory, and anti-apoptotic mechanisms. J Funct Foods 2023;102(January). https://doi.org/10.1016/j.jff.2023.105461.
[19] Li R, Chen J, Li H, Zhang Z, Tang H. Effects of calcium ions on the particle performance of luteolin-loaded zein-gum arabic-tea polyphenols ternary complex nanoparticles. Lwt 2023;184(January):115057. https://doi.org/10.1016/j.lwt.2023.115057.
[20] Shinde P, Agraval H, Singh A, Yadav UCS, Kumar U. Synthesis of luteolin loaded zein nanoparticles for targeted cancer therapy improving bioavailability and efficacy. J Drug Deliv Sci Technol 2019;52(April):369–78. https://doi.org/10.1016/j.jddst.2019.04.044.
[21] Roya S, Abbastabar M, Nosratabadi M. High antimicrobial, cytotoxicity, and catalytic activities of biosynthesized selenium nanoparticles using Crocus caspius extract. Arab J Chem 2023;16(6):104705. https://doi.org/10.1016/j.arabjc.2023.104705.
[22] Alhazza IM, Ebaid H, Omar MS, Hassan I. Supplementation with selenium nanoparticles alleviates diabetic nephropathy during pregnancy in the diabetic female rats. 2021.
[23] Ramamurthy CH, Sampath KS, Arunkumar P, Kumar MS, Sujatha V, Premkumar K, et al. Green synthesis and characterization of selenium nanoparticles and its augmented cytotoxicity with doxorubicin on cancer cells. Bioproc Biosyst Eng 2013;36(8):1131–9. https://doi.org/10.1007/s00449-012-0867-1.
[24] Sakr TM, Korany M, Katti KV. Selenium nanomaterials in biomedicine—an overview of new opportunities in nanomedicine of selenium. J Drug Deliv Sci Technol 2018;46(April):223–33. https://doi.org/10.1016/j.jddst.2018.05.023.
[25] Jia X, Liu Q, Zou S, Xu X, Zhang L. Construction of selenium nanoparticles/β-glucan composites for enhancement of the antitumor activity. Carbohydr Polym 2015;117:434–42. https://doi.org/10.1016/j.carbpol.2014.09.088.
[26] Song X, Qiao L, Yan S, Chen Y, Dou X, Xu C. Preparation, characterization, and in vivo evaluation of anti-inflammatory activities of selenium nanoparticles synthesized by Kluyveromyces lactis GG799. Food Funct 2021;12(14):6403–15. https://doi.org/10.1039/d1fo01019k.
[27] Chen YY, Liu K, Zha XQ, Li QM, Pan LH, Luo JP. Encapsulation of luteolin using oxidized lotus root starch nanoparticles prepared by anti-solvent precipitation. Carbohydr Polym 2021;273(April):118552. https://doi.org/10.1016/j.carbpol.2021.118552.
[28] Cittrarasu V, Kaliannan D, Dharman K, Maluventhen V, Easwaran M, Liu WC, et al. Green synthesis of selenium nanoparticles mediated from Ceropegia bulbosa Roxb extract and its cytotoxicity, antimicrobial, mosquitocidal and photocatalytic activities. Sci Rep Dec 2021;11(1). https://doi.org/10.1038/s41598-020-80327-9.
[29] Diko CS, Zhang H, Lian S, Fan S, Li Z, Qu Y. Optimal synthesis conditions and characterization of selenium nanoparticles in Trichoderma sp. WL-Go culture broth. Mater Chem Phys May 2020;246. https://doi.org/10.1016/j.matchemphys.2019.122583.
[30] Ahmed MK, Moydeen AM, Ismail AM, El-Naggar ME, Menazea AA, El-Newehy MH. Wound dressing properties of functionalized environmentally biopolymer loaded with selenium nanoparticles. J Mol Struct 2021;1225:129138. https://doi.org/10.1016/j.molstruc.2020.129138.
[31] Kumar M, Dwivedi C, Shah CP, Singh K, Bajaj PN. An organic acid-induced synthesis and characterization of selenium nanoparticles. J Nanotechnol 2011. https://doi.org/10.1155/2011/651971.
[32] Qi W, Cai P, Yuan W, Wang H. Tunable swelling of polyelectrolyte multilayers in cell culture media for modulating NIH-3T3 cells adhesion. J Biomed Mater Res 2014;102(11):4071–7. https://doi.org/10.1002/jbm.a.35094.
[33] Andersson AK, Sandler S. Melatonin protects against streptozotocin, but not interleukin-1β-induced damage of rodent pancreatic β-cells. J Pineal Res 2001;30(3):157–65. https://doi.org/10.1034/j.1600-079X.2001.300304.x.
[34] Yu Q, Zhang M, Qian L, Wen D, Wu G. Luteolin attenuates high glucose-induced podocyte injury via suppressing NLRP3 inflammasome pathway. Life Sci 2019;225(January):1–7. https://doi.org/10.1016/j.lfs.2019.03.073.
[35] Song S, An J, Li Y, Liu S. Electroacupuncture at ST-36 ameliorates DSS-induced acute colitis via regulating macrophage polarization induced by suppressing NLRP3/IL-1β and promoting Nrf2/HO-1. Mol Immunol 2019;106(1277):143–52. https://doi.org/10.1016/j.molimm.2018.12.023.
[36] Zhang ZH, Liu JQ, Hu CD, Zhao XT, Qin FY, Zhuang Z, et al. Luteolin confers cerebroprotection after subarachnoid hemorrhage by suppression of NLPR3 inflammasome activation through Nrf2-dependent pathway. Oxid Med Cell Longev 2021;2021. https://doi.org/10.1155/2021/5838101.
[37] Yang Y, Song Z, Wu W, Xu A, Lv S, Ji S. ZnO quantum dots induced oxidative stress and apoptosis in HeLa and HEK-293T cell lines. Front Pharmacol 2020;11(February):1–8. https://doi.org/10.3389/fphar.2020.00131.
[38] Mostafa AM. Preparation and study of nonlinear response of embedding ZnO nanoparticles in PVA thin film by pulsed laser ablation. J Mol Struct 2021;1223. https://doi.org/10.1016/j.molstruc.2020.129007.
[39] Dang H, Meng MH, Zhao H, Iqbal J, Dai R, Deng Y, et al. Luteolin-loaded solid lipid nanoparticles synthesis, characterization, & improvement of bioavailability, pharmacokinetics in vitro and vivo studies. J Nanoparticle Res 2014;16(4). https://doi.org/10.1007/s11051-014-2347-9.
[40] Waghmare AS, Grampurohit ND, V Gadhave M, Gaikwad DD, Jadhav SL. Issn 2230 – 8407 solid lipid nanoparticles: a promising. Drug Deliv Syst 2012;3(4):100–7.
[41] Zou X, Jiang Z, Li L, Huang Z. Selenium nanoparticles coated with pH responsive silk fibroin complex for fingolimod release and enhanced targeting in thyroid cancer. Artif Cells Nanomed Biotechnol 2021;49(1):83–95. https://doi.org/10.1080/21691401.2021.1871620.
[42] Tang S, Wang T, Jiang M, Huang C. PT NU SC. Int J Biol Macromol 2019. https://doi.org/10.1016/j.ijbiomac.2019.01.152. #pagerange#.
[43] Jurasekova Z, Marconi G, Sanchez-Cortes S, Torreggiani A. Spectroscopic and molecular modeling studies on the binding of the flavonoid luteolin and human serum albumin. Biopolymers 2009;91(11):917–27. https://doi.org/10.1002/bip.21278.
[44] Alagesan V, Venugopal S. Green synthesis of selenium nanoparticle using leaves extract of Withania somnifera and its biological applications and photocatalytic activities. Bionanoscience 2019;9(1):105–16. https://doi.org/10.1007/s12668-018-0566-8.
[45] Zou N, Wang X, Li G. Spectroscopic and electrochemical studies on the interaction between luteolin and DNA. J Solid State Electrochem 2016;20(6):1775–82. https://doi.org/10.1007/s10008-016-3174-y.
[46] Gutiérrez RMP, Gómez JT, Urby RB, Soto JGC, Parra HR. Evaluation of diabetes effects of selenium nanoparticles synthesized from a mixture of luteolin and Diosmin on Streptozotocipe 2 diabetes in mice. Molecules 2022;27(17). https://doi.org/10.3390/molecules27175642.
[47] Gutiérrez RMP, Gómez JT, Jerónimo FFM, Paredes-Carrera SP, Sánchez-Ochoa JC. Effects of selenium nanoparticles using potential natural compounds Naringenin and Baicalin for diabetes. Biointerface Res Appl Chem 2023;13(6):1–18. https://doi.org/10.33263/BRIAC136.597.
[48] Chakra CS, Divya V, Shireesha K, Madhuri S, Rakesh Kumar T, Uday Krishna A, et al. In: Synthesis and characterization of emerging nanomaterials. Emerging

materials: design, characterization and applications. Springer Singapore; 2022. p. 37–102. https://doi.org/10.1007/978-981-19-1312-9_2.
[49] Hsu CL, Yen GC. Induction of cell apoptosis in 3T3-L1 pre-adipocytes by flavonoids is associated with their antioxidant activity. Mol Nutr Food Res 2006;50(11):1072–9. https://doi.org/10.1002/mnfr.200600040.
[50] Lei H, Han J, Wang Q, Guo S, Sun H, Zhang X. Effects of sesamin on streptozotocin (STZ)-induced NIT-1 pancreatic β-cell damage. Int J Mol Sci 2012;13(12):16961–70. https://doi.org/10.3390/ijms131216961.
[51] Liu K, cheng Liu P, Liu R, Wu X. Dual AO/EB staining to detect apoptosis in osteosarcoma cells compared with flow cytometry. Med Sci Monit Basic Res 2015;21:15–20. https://doi.org/10.12659/MSMBR.893327.
[52] Marvibaigi M, Amini N, Supriyanto E, Abdul Majid FA, Kumar Jaganathan S, Jamil S, et al. Antioxidant activity and ROS-dependent apoptotic effect of scurrula ferruginea (jack) danser methanol extract in human breast cancer cell MDA-MB-231. PLoS One 2016;11(7):1–36. https://doi.org/10.1371/journal.pone.0158942.
[53] Yu JB, et al. Role of Nrf2/ARE pathway in protective effect of electroacupuncture against endotoxic shock-induced acute lung injury in rabbits. PLoS One 2014;9(8). https://doi.org/10.1371/journal.pone.0104924.
[54] Kryl'skii ED, Popova TN, Safonova OA, Stolyarova AO, Razuvaev GA, de Carvalho MAP. Transcriptional regulation of antioxidant enzymes activity and modulation of oxidative stress by melatonin in rats under cerebral ischemia/reperfusion conditions. Neuroscience 2019;406:653–66. https://doi.org/10.1016/j.neuroscience.2019.01.046.
[55] Bai J, Wang Y, Zhu X, Shi J. Eriodictyol inhibits high glucose-induced extracellular matrix accumulation, oxidative stress, and inflammation in human glomerular mesangial cells. Phytother Res 2019;33(10):2775–82. https://doi.org/10.1002/ptr.6463.
[56] Chen L, Tian G, Tang W, Luo W, Liu P, Ma Z. Protective effect of luteolin on streptozotocin-induced diabetic renal damage in mice via the regulation of RIP140/NF-κB pathway and insulin signalling pathway. J Funct Foods 2016;22:93–100. https://doi.org/10.1016/j.jff.2016.01.023.
[57] Lv D, Zhou Q, Xia Y, You X, Zhao Z, Li Y, et al. The association between oxidative stress alleviation via sulforaphane-induced Nrf2-HO-1/NQO-1 signaling pathway activation and chronic renal allograft dysfunction improvement. Kidney Blood Press Res 2018;43(1):191–205. https://doi.org/10.1159/000487501.
[58] Singh R, Avliyakulov NK, Braga M, Haykinson MJ, Martinez L, Singh V, et al. Proteomic identification of mitochondrial targets of arginase in human breast cancer. PLoS One 2013;8(11):1–15. https://doi.org/10.1371/journal.pone.0079242.
[59] Al-Nahdi AMT, John A, Raza H. Cytoprotective effects of N-acetylcysteine on streptozotocin-induced oxidative stress and apoptosis in RIN-5F pancreatic β-cells. Cell Physiol Biochem 2018;51(1):201–16. https://doi.org/10.1159/000495200.
[60] Gomes A, Fernandes E, Lima JLFC. Fluorescence probes used for detection of reactive oxygen species. J Biochem Biophys Methods 2005;65(2–3):45–80. https://doi.org/10.1016/j.jbbm.2005.10.003.
[61] Tao T, Liu GJ, Shi X, Zhou Y, Lu Y, Gao YY, et al. DHEA attenuates microglial activation via induction of JMJD3 in experimental subarachnoid haemorrhage. J Neuroinflammation 2019;16(1):1–14. https://doi.org/10.1186/s12974-019-1641-y.
[62] Cheng T, Wang W, Li Q, Han X, Xing J, Qi C, et al. Cerebroprotection of flavanol (-)-epicatechin after traumatic brain injury via Nrf2-dependent and-independent pathways. Free Rad Biol Med 2016 Mar 1;92:15–28.
[63] You BR, Moon HJ, Han YH, Park WH. Gallic acid inhibits the growth of HeLa cervical cancer cells via apoptosis and/or necrosis. Food Chem Toxicol 2010;48(5):1334–40. https://doi.org/10.1016/j.fct.2010.02.034.
[64] Cadenas S. Mitochondrial uncoupling, ROS generation and cardioprotection. Biochim Biophys Acta Bioenerg 2018;1859(9):940–50. https://doi.org/10.1016/j.bbabio.2018.05.019.
[65] Yang F, Tang Q, Zhong X, Bai Y, Chen T, Zhang Y, et al. Surface decoration by Spirulina polysaccharide enhances the cellular uptake and anticancer efficacy of selenium nanoparticles. Int J Nanomed 2012;7:835–44. https://doi.org/10.2147/IJN.S28278.
[66] Bauernfeind F, Bartok E, Rieger A, Franchi L, Núñez G, Hornung V. Cutting edge: reactive oxygen species inhibitors block priming, but not activation, of the NLRP3 inflammasome. J Immunol 2011;187(2):613–7. https://doi.org/10.4049/jimmunol.1100613.